UV SERS at well ordered Pd sphere segment void (SSV) nanostructures

L. Cui,[a] S. Mahajan,[b] R. M. Cole,[c] B. Soares,[c] P. N. Bartlett,[b] J. J. Baumberg,[c] I. P. Hayward,[d] B. Ren,[a] A. E. Russell*[b] and Z. Q. Tian[a]

Received 9th October 2008, Accepted 4th December 2008
First published as an Advance Article on the web 18th December 2008
DOI: 10.1039/b817803h

Ultraviolet laser excited surface-enhanced Raman scattering was obtained for the first time at the well ordered palladium sphere segment void (SSV) nanostructures, using adenine as the probe molecule, and the UV-SERS enhancement is found to be correlated well with the plasmon absorption of Pd SSVs in the UV region.

Surface enhanced Raman spectroscopy has been widely used in various analytical applications.[1–3] Most SERS studies utilise visible or near-infrared excitation; use of UV excitation is still relatively unexplored despite offering important advantages. Firstly, UV energies are in pre-resonance or full resonance with the electronic absorption of many molecules, such as biomolecules (nucleic acids and proteins), organic molecules and inorganic materials,[4,5] so that if the substrates support electromagnetic (EM) enhancements in the UV region, both the resonance Raman effect and SERS effect will be excited by the UV laser, resulting in UV-SERRS with high detection sensitivity. In addition, UV excitation can provide a fluorescence-free background and higher spatial resolution; extremely useful for the investigation of biological, medical, catalytic systems and for materials science applications.[6,7]

Although many groups have tried to obtain SERS in the UV region, successful reports are still very rare, indicating the much greater difficulties encountered in obtaining UV-SERS than with visible or NIR laser excited SERS. Coinage metal nanostructures exhibit extremely strong enhancements in the visible region, but the enhancement decreases sharply to an unobservable level in the UV region, due to the damping of the surface-plasmon resonance by the strong interband transition absorption in the UV region.[8,9] UV-SERS has been obtained on Rh, Co, Ru and Al transition metal nanostructures, fabricated by electrochemical oxidation-reduction cycles, electrodeposition or magnetron sputtering,[9–11] indicating the different optical properties of these transition metals from coinage metals. However, we still fail to get UV-SERS active substrates on other transition metals such as Pd, a very important catalytic metal, using these traditional fabrication methods. To propel the development of UV-SERS, novel nanostructure fabrication methods look to be promising. In addition, the origin of the enhancement in the UV region has never been experimentally explored, although there are some preliminary theoretical calculations,[11,12] and use of such ordered structures should make such exploration more facile.

In the study reported here, templated electrodeposition through colloidal sphere templates will be used to produce well ordered Pd sphere segment void (SSV) nanostructures consisting of hexagonal close-packed arrays of uniform sphere segment cavities. A great advantage of this substrate is that both the template sphere diameter and film thickness can be conveniently varied to control the optical properties of the substrates. The surfaces can, therefore, be precisely tailored to tune the surface plasmons that give rise to the optimal SERS enhancements, as demonstrated in the visible and near-IR regions at such gold, palladium and platinum SSV substrates.[13–16] Similarly, this kind of reliable and reproducible SERS substrate should facilitate the experimental exploration of UV-SERS and a comprehensive understanding of the enhancement mechanisms in the UV region.

We fabricated a series of SERS substrates by electrodeposition of Pd through colloidal templates with polystyrene sphere diameters from 200–800 nm to seek the best enhancements with 325 nm excitation. The substrates were gradually removed from the plating bath in steps of 1 mm to provide graduations in the Pd SSV film thickness across the sample as fractions of the sphere diameter, *D*. Fig. 1 shows the SEM image (Jeol JSM 6500 FESEM) of a Pd SSV film templated by 200 nm diameter spheres. We note that there are no previous reports of such large areas of monolayer assemblies using spheres with such a small diameter. SEM images from other sizes of sphere can be found elsewhere.[14]

Surface plasmon absorption spectra, obtained using normal incidence reflectance measurements (Jasco V-570 UV/Vis/NIR spectrophotometer) and normalised with respect to that of a flat palladium film produced by evaporation onto a glass slide,

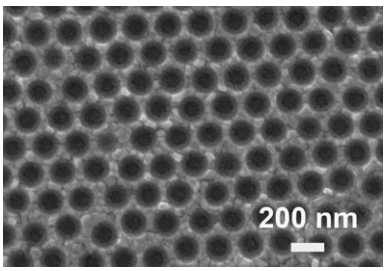

Fig. 1 SEM image of the Pd SSV film produced using 200 nm diameter template spheres with the thickness of 0.3 D.

[a] *State Key Laboratory of Physical Chemistry of Solid Surface and Department of Chemistry, Xiamen University, Xiamen 361005, China. E-mail: zqtian@xmu.edu.cn; Fax: +86 592 2085349; Tel: +86 592 2186979*
[b] *School of Chemistry, University of Southampton, Southampton, UK SO17 1BJ. E-mail: a.e.russell@soton.ac.uk; Fax: +44 23 8059 3781; Tel: +44 23 8059 3306*
[c] *School of Physics, University of Southampton, Southampton, UK SO17 1BJ*
[d] *Renishaw plc, Old Town, Wotton-under-Edge, Gloucestershire, UK GL12 7DW. E-mail: ian.hayward@renishaw.com; Fax: +44 1453 523800; Tel: +44 1453 523833*

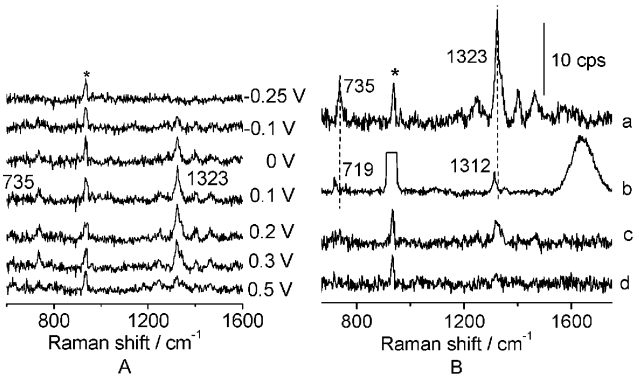

Fig. 2 (A) Potential dependent UV-SERS spectra of adenine adsorbed on the structured palladium film produced using 200 nm diameter template spheres in 1 mM adenine + 0.1 M $HClO_4$. (B) SERS spectra of adenine on (a) a Pd SSV film templated by 200 nm diameter spheres at 0.1 V, (b) Raman spectra from the solution of 1 mM adenine + 0.1 M $HClO_4$, (c) SERS at an electrodeposited Pd film without templates at 0.1 V, and (d) SERS at an evaporated Pd film at 0.1 V. The 933 cm^{-1} band marked with * is from the symmetric stretching vibration of ClO_4^- in the electrolyte solution.

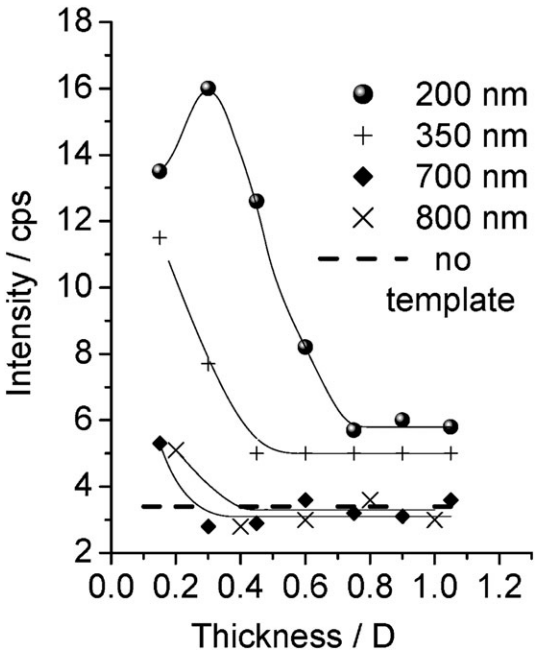

Fig. 3 Thickness dependent SERS intensity of the peak at 1323 cm^{-1} obtained at graded Pd SSV films templated by 200, 350, 700 and 800 nm diameter spheres and a film electrodeposited onto the flat evaporated Pd film without a template.

were acquired to aid understanding of the enhancement mechanism(s). The illuminated area was restricted to 750 μm × 4 mm so as to ensure that only one film thickness (step) was illuminated. Because the plasmon bands shift with the dielectric constant of the external medium,[17] reflectance spectra were also acquired in the aqueous medium to be consistent with the SERS measurements. All the Raman spectra were recorded using a Renishaw inVia Raman microscope using a 325 nm HeCd laser with 3 mW laser power at the sample, a 15× UV objective (NA 0.32, WD 8.5 mm from OFR Inc.) and a 50 s accumulation time. A spectro-electrochemical cell with a three-electrode configuration was used during Raman measurements. All the potentials are quoted *vs.* SCE.

Fig. 2 shows a set of the UV-SERS spectra of the protonated adenine molecules adsorbed on the Pd SSV film at different potentials in 1 mM adenine + 0.1 M $HClO_4$. The spectra were corrected by removal of the contribution from solution species based on the intensity of the water band at 1630 cm^{-1}, which is clearly seen in the spectrum of the adenine solution (Fig. 2B, spectrum b). The intensity is potential dependent and reaches a maximum at 0.1–0.2 V. Thus, a potential of 0.1 V was applied for the subsequent comparisons of the UV-SERS for the series of Pd SSV substrates. The bands at 735 and 1323 cm^{-1} are characteristic bands of adenine and are assigned to the ring breathing vibration of the whole molecule and the C–H in-plane bending mode.[18]

Compared with the Raman spectrum of adenine solution, significant shifts can be observed in the SERS bands (Fig. 2B, spectrum a), *i.e.* the bands at 719 and 1312 cm^{-1} in the SERS spectrum shift to 735 and 1323 cm^{-1} in the solution spectrum. Moreover, the relative intensities of these two bands are different. These observations confirm that the UV-SERS spectra are indeed from the adsorbed species and the Pd SSV substrates are UV-SERS active.

UV-SERS spectra of adenine adsorbed at 0.1 V were also acquired on the other Pd SSVs. Fig. 3 shows the intensity of the 1323 cm^{-1} band as a function of the thickness of palladium SSV films prepared with 200, 350, 700 and 800 nm diameter template spheres. The intensities vary with the film thickness and diameter of sphere and, therefore, we attribute the enhancement to specific features of the SSV structure. Significant enhancements were only observed for the films prepared using the 200 and 350 nm spheres and only for the thinner films. For Pd SSV films using 700 and 800 nm spheres, the SERS intensity is almost independent of film thickness and sphere diameter, except that a slightly stronger signal is observed for the thinnest films. The maximum UV-SERS intensity is observed at the 200 nm sphere templated SSV film for the film thickness of 0.3 D. This is in contrast to the results previously reported for 633 nm excitation, in which the best enhancements were obtained for Pd SSV film templated by 600 nm spheres at around 0.8 D,[14] indicating that, as expected, the optimal substrate is different for different excitation lines. The enhancement factor (EF) of the best Pd SSV film for UV-SERS, *i.e.* 200 nm spheres at 0.3 D, was found to be approximately 150, which is similar to that reported for electrochemically roughened Rh electrodes with 325 nm excitation by Ren *et al.*[11]

The surface area of the SSV substrates relative to that of a smooth metal surface, R, is related to the sphere radius, r, and the film thickness, D, as follows.

$$R = 1 + \frac{2\pi}{\sqrt{3}} D^2$$

Thus, the maximum increase in surface area is 3.6× that of the smooth surface. Therefore, the 150× enhancement observed is not simply accounted for by the increase in surface area and corresponding increase in number of adsorbate molecules in the spot defined by the laser. In previous studies of such

surfaces,[19] we have found an R value from the electrochemical stripping of an adsorbed oxide film on Au structures with D = 0.67 of 1.6, in agreement with the theoretical value, confirming that the deposited surfaces are smooth.

To add further confirmation that the observed enhancements did not originate from any inherent roughness of the metal deposit, we also obtained spectra of adenine adsorbed at Pd films electrodeposited in the absence of the colloidal templates with a variety of film thicknesses, from 40–720 nm (Fig. 2B, spectrum c) and on an evaporated Pd film (Fig. 2B, spectrum d). No UV-SERS signal was detected at the evaporated Pd film. However, the Pd films electrodeposited without templates yielded a UV-SERS signal, the intensity of which did not vary with the film thickness. This intensity was very similar to that obtained from Pd SSVs templated by 700 and 800 nm spheres (dashed line, Fig. 3) and represents and enhancement factor of approximately 33×.

Attaining the optimal SERS enhancement at such SSV substrates depends upon matching of the incident and the scattered radiation with the plasmon absorption of the substrate. To relate the dependence of the UV-SERS enhancements to the plasmon absorption of the structured film, reflectance spectra were recorded on the 200 and 800 nm stepped Pd SSV surfaces in aqueous medium (Fig. 4A and B). The reflectance spectrum obtained for the film deposited without a template is also shown as the dashed line in Fig. 4B. Dips in the reflectivity, corresponding to plasmon absorptions, vary in position with the film thickness. The wavelengths corresponding to the laser excitation at 325 nm and the Stokes scattered radiation at 340 nm corresponding to the 1323 cm^{-1} peak of adsorbed adenine, are indicated by the vertical dashed lines in Fig. 4.

The surface plasmon modes that contribute to the features observed in reflectance spectra from such truncated spherical cavity substrates are formed from both propagating Bragg modes, corresponding to plasmons on the upper flat surface around the voids, and localized Mie modes, corresponding to plasmons trapped in the spherical cavities.[20] As previously discussed, the Bragg modes dominate for the thinnest films and the Mie modes begin to contribute as the thickness increases and dominate the spectrum around 0.7 D. As the thickness is increased, interference between the two modes may be observed. The presence of both modes is apparent in the reflectance spectra shown in Fig. 4. The absorbance at shorter wavelengths in the spectra of the thinnest 200 nm films is attributed to the Bragg modes, the position of which does not change as the film thickness is increased. As the thickness is increased, a second feature is observed, the maximum of which shifts to longer wavelength as the film thickness is increased. The spacing between the shallow dishes formed on the surface for the thinner 800 nm films does not yield as efficient Bragg scattering as that for the 200 nm films and, thus, the reflectance spectra are relatively featureless for the 0.2 and 0.4 D 800 nm films. The reflectance spectra from the thicker 800 nm sphere templated surfaces show many higher order surface plasmon mixed modes as the relative areas of the top surface and cavities vary.

As can be seen in Fig. 4a, for the 200 nm sphere templated film, both the wavelength of the excitation laser and Raman scattered photons have a better overlap with the strong absorption in the reflectance spectra for the thinner film, which accounts for the larger SERS signal. The 800 nm and non-templated films studied all show similar weak absorbance in the 325–400 nm region, explaining the similar SERS intensities observed. Additionally, it is well-known that the EF is inversely proportional to the fourth power of the surface plasmon linewidth.[21,22] The plasmon absorption band of 800 nm Pd SSV films is broader in the UV range than that of 200 nm Pd SSV films, implying they have a smaller EF and thus accounting for the stronger signal observed on the latter.

Although the UV-SERS intensities reported here and previously are still relatively low compared with visible-SERS, it should be mentioned that many optical elements in the Raman spectrometer have much lower performance in the UV than in the visible region, *e.g.* the quantum efficiency of CCD and throughput of Raman spectrometer. Using a quantitative comparison and, provided that the performance of Raman spectrometer is the same in the UV and visible region, we predict that the UV-SERS intensity will be stronger than visible-SERS.

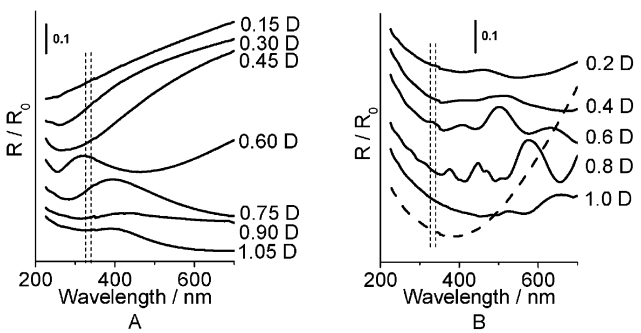

Fig. 4 Normal incidence reflectance spectra for graded, Pd SSV films grown through the (A) 200 nm and (B) and 800 nm diameter template spheres in 0.1 M $HClO_4$ aqueous solution. The spectrum obtained for the film electrodeposited without the template is shown in (B) as the thick dashed line. The thin dashed vertical lines denote the laser excitation at 325 nm and the Stokes scattered photons at 340 nm corresponding to the 1323 cm^{-1} peak of adsorbed adenine. The scale is linear and the spectra have been offset for clarity.

Conclusions

In summary, we report the first UV-SERS enhancement at a Pd SSV film surface. The origins of the enhancement for adenine adsorbed on the Pd surface are clearly attributed to the unique plasmonic behaviour of the SSV structure in the UV region. The best UV-SERS enhancement (an enhancement factor of 150) is observed for 200 nm diameter 0.3 D thick Pd SSV film.

Acknowledgements

The assistance of Tim Smith and Matthew Bloomfield at Renishaw are gratefully acknowledged. The work was supported by the EPSRC (EP/C511786/1 and EP/F059396/1), Renishaw, and the NSFC (20433040).

References

1 K. Kneipp, H. Kneipp and M. Moskovits, *Surface-Enhanced Raman Scattering: Physics and Applications*, Springer GmbH, Berlin, 2006.
2 K. Hering, D. Cialla, K. Ackermann, T. Dörfer, R. Möller, H. Schneidewind, R. Mattheis, W. Fritzsche, P. Rösch and J. Popp, *Anal. Bioanal. Chem.*, 2008, **390**, 113.
3 K. Kneipp, H. Kneipp, I. Itzkan, R. R. Dasari and M. S. Feld, *Chem. Rev.*, 1999, **99**, 2957.
4 S. A. Asher, *Anal. Chem.*, 1993, **65**, 201A.
5 S. P. A. Fodor and T. G. Spiro, *J. Am. Chem. Soc.*, 1986, **108**, 3198.
6 P. C. Stair and C. Li, *J. Vac. Sci. Technol., A*, 1997, **15**, 1679.
7 V. Pajcini, C. H. Munro, R. W. Bormett, R. E. Witkowski and S. A. Asher, *Appl. Spectrosc.*, 1997, **51**, 81.
8 D. M. Kolb, in *Spectroelectrochemistry: Theory and Practice*, ed. R. J. Gale, Plenum, New York, 1988, vol. 4, p. 92.
9 Z. Q. Tian, Z. L. Yang, B. Ren and D. Y. Wu, *Top. Appl. Phys.*, 2006, **103**, 125.
10 T. Doerfer, M. Schmitt and J. Popp, *J. Raman Spectrosc.*, 2007, **38**, 1379.
11 B. Ren, X. F. Lin, Z. L. Yang, G. K. Liu, R. F. Aroca, B. W. Mao and Z. Q. Tian, *J. Am. Chem. Soc.*, 2003, **125**, 9598.
12 D. P. DiLella, A. Gohin, R. H. Lipson, P. McBreen and M. Moskovits, *J. Chem. Phys.*, 1980, **73**, 4282.
13 S. Mahajan, J. J. Baumberg, A. E. Russell and P. N. Bartlett, *Phys. Chem. Chem. Phys.*, 2007, **9**, 6016.
14 M. E. Abdelsalam, S. Mahajan, P. N. Bartlett, J. J. Baumberg and A. E. Russell, *J. Am. Chem. Soc.*, 2007, **129**, 7399.
15 S. Cintra, M. E. Abdelsalam, P. N. Bartlett, J. J. Baumberg, T. A. Kelf, Y. Sugawara and A. E. Russell, *Faraday Discuss.*, 2006, **132**, 191.
16 P. N. Bartlett, J. J. Baumberg, S. Coyle and M. E. Abdelsalam, *Faraday Discuss.*, 2004, **125**, 117.
17 A. J. Haes, L. Chang, W. L. Klein and R. P. Van Duyne, *J. Am. Chem. Soc.*, 2005, **127**, 2264.
18 Y. Xue, D. Xie and G. Yan, *Int. J. Quantum Chem.*, 2000, **76**, 686.
19 M. E. Abdelsalam, P. N. Bartlett, J. J. Baumberg, S. Cintra, T. A. Kelf and A. E. Russell, *Electrochem. Commun.*, 2005, **7**, 740.
20 T. A. Kelf, Y. Sugawara, R. M. Cole, J. J. Baumberg, M. E. Abdelsalam, S. Cintra, S. Mahajan, A. E. Russell and P. N. Bartlett, *Phys. Rev. B: Condens. Matter Mater. Phys.*, 2006, **74**, 245415/1.
21 U. Kreibig and M. Vollmer, *Optical properties of metal clusters*, Springer, Berlin, Germany, 1995.
22 F. Stietz, J. Bosbach, T. Wenzel, T. Vartanyan, A. Goldmann and F. Trager, *Phys. Rev. Lett.*, 2000, **84**, 5644.

